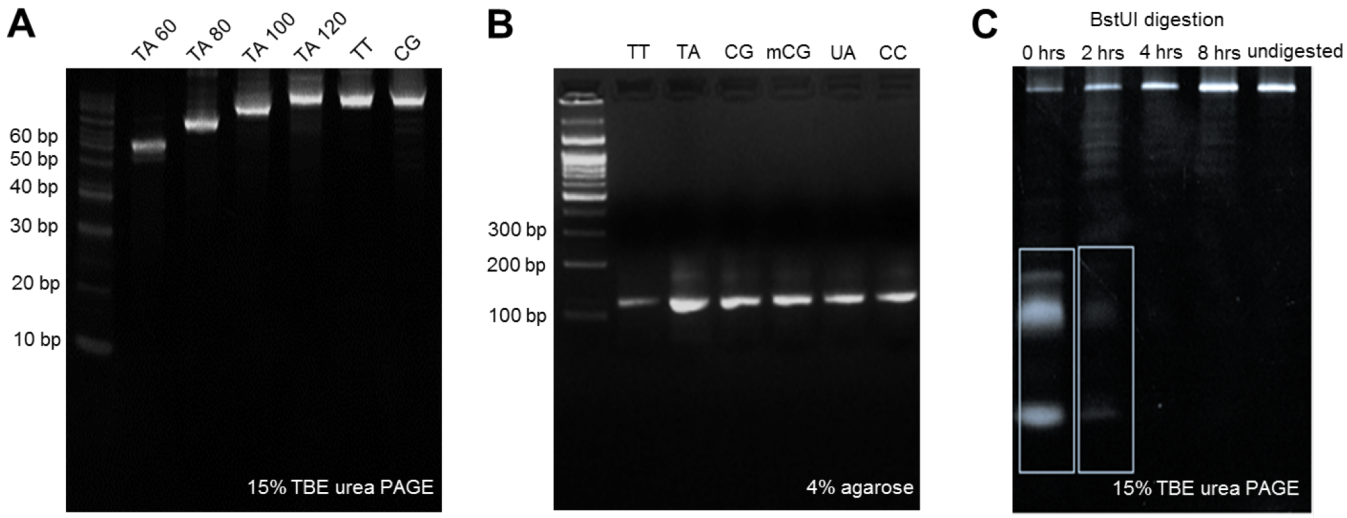


**Supplementary Figure 1.** Verification of the DNA constructs by gel electrophoresis. All gels were stained with SyBr gold and imaged with 535 nm excitation. **(A, B)** Gel electrophoresis of TA-rich DNAs with varying length and TT-rich, CG-rich, $^{m}$CG-rich, UA-rich, and CC-rich DNA constructs, either under denaturing condition on 15% TBE urea polyacrylamide gel with formamide-denatured DNA (A) or under native condition on 4% agarose gel (B). **(C)** BstUI digestion of mCG-rich DNA construct methylated by M.SssI methyltransferase enzyme for the marked time. Digested fragments disappeared after 4 hours of methylation. DNA construct was used for experiments after 8 hours of methylation.

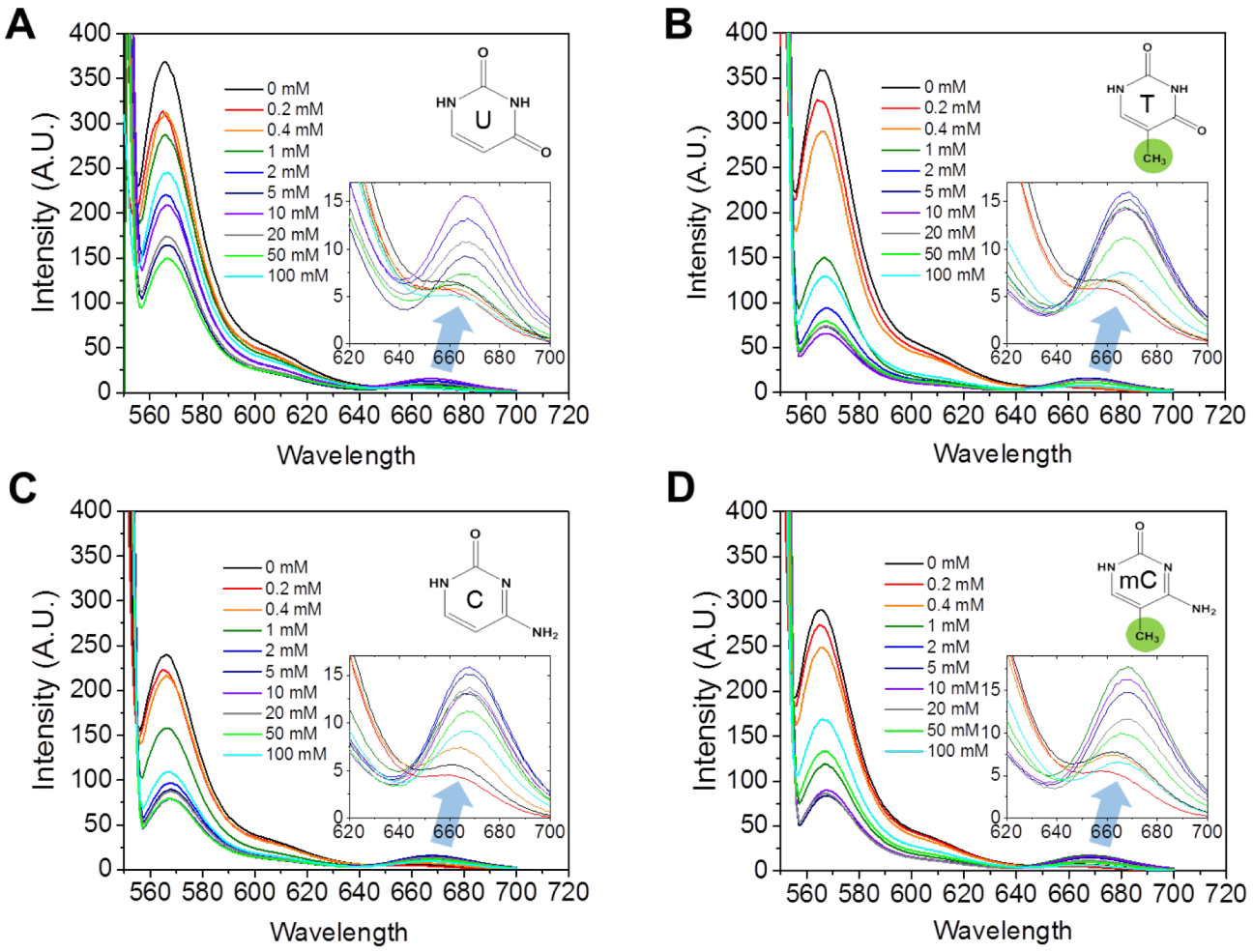


**Supplementary Figure 2.** Emission spectra from FRET measurement on UA-rich (A), TA-rich (B), CG-rich (C), and $^{m}$CG-rich (D) DNA constructs, showing two peaks corresponding to Cy3 (568 nm) and Cy5 (668 nm) emission. Insets show the zoomed-in spectra around Cy5 emission.

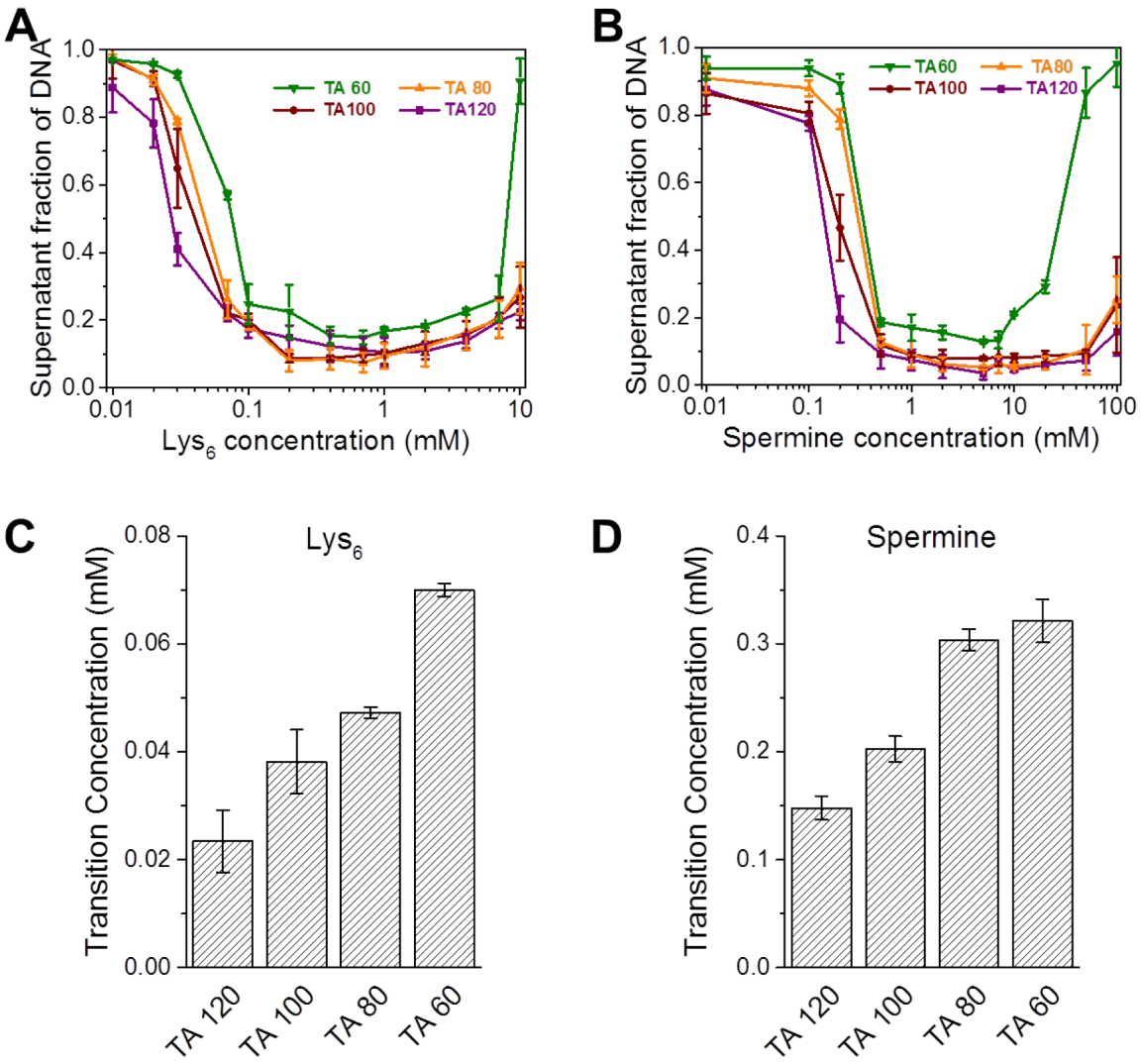


**Supplementary Figure 3.** Precipitation measurement on TA-rich DNA constructs with varying length (60, 80, 100, and 120 bp) with $Lys_6$ (A) or spermine (B). Transition concentration of the precipitation gradually increases with decreasing DNA length commonly for both kinds of polycations (C and D).

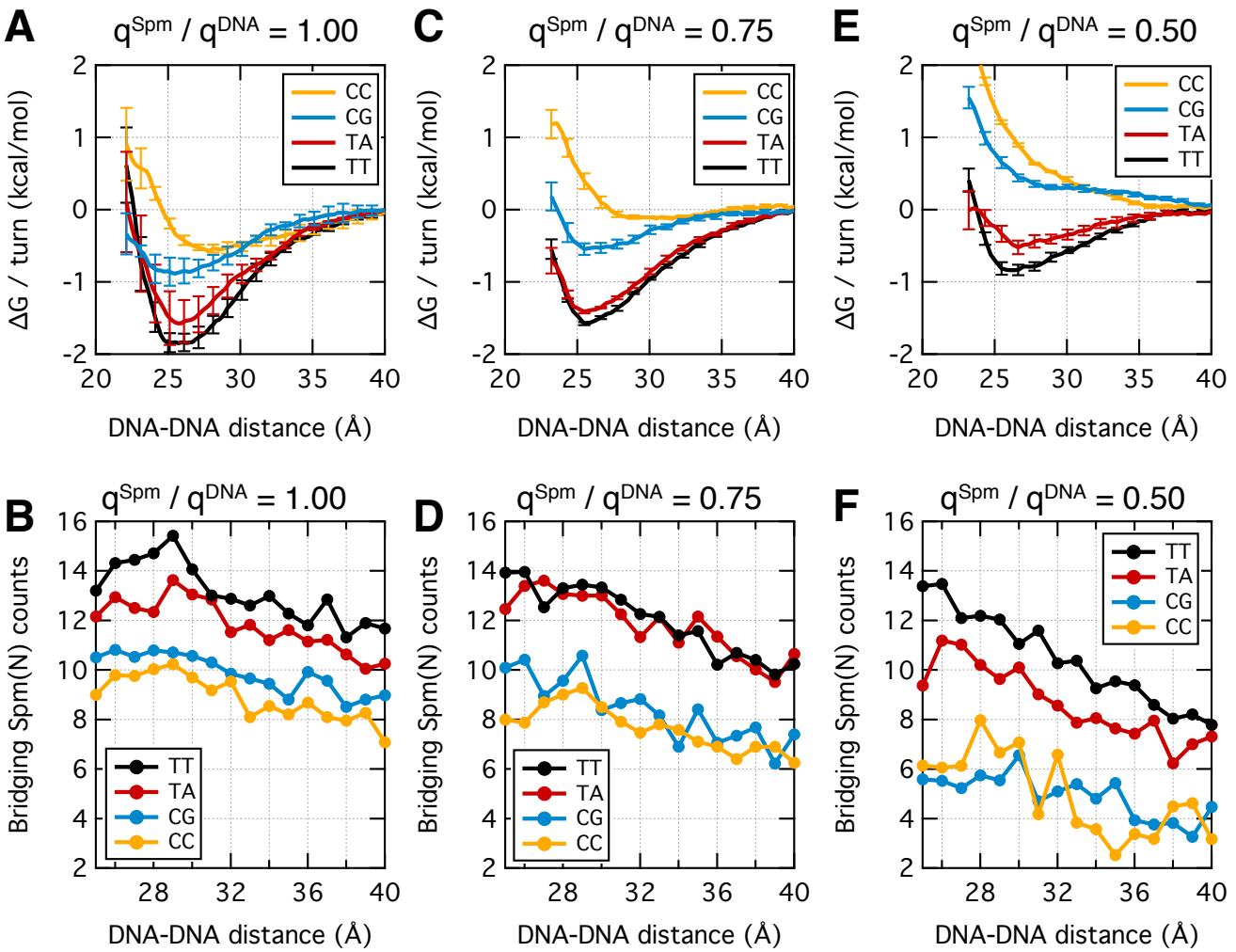


**Supplementary Figure 4.** Sequence dependence of the interaction free energy and spermine bridging between a pair of DNA molecules of identical sequences in MD simulations at three different ratios of total spermine charge ($q^{Spm}$) to total DNA charge ($q^{DNA}$): $q^{DNA}$ / $q^{DNA}$ = 1.00 (A,B), 0.75 (C,D), and 0.50 (E,F). When spemine does not fully neutralize the DNA charges, the charge neutrality was achieved by adding Na ions. For all simulations, an explicit solution of 100 nM NaCl was used. **(A,C,E)** Interaction free energy between two dsDNA molecules as a function of inter-DNA distance. **(B,D,F)** The count of bridging spermine nitrogen atoms, computed by integrating the local concentration heatmaps over $x$ = [–$d$/2+10 Å, $d$/2–10 Å] and $y$ = [–10 Å, 10 Å], as a function of $d$. Note that panels A and B are taken from Yoo *et al.*, Nat. Comm. (2017).

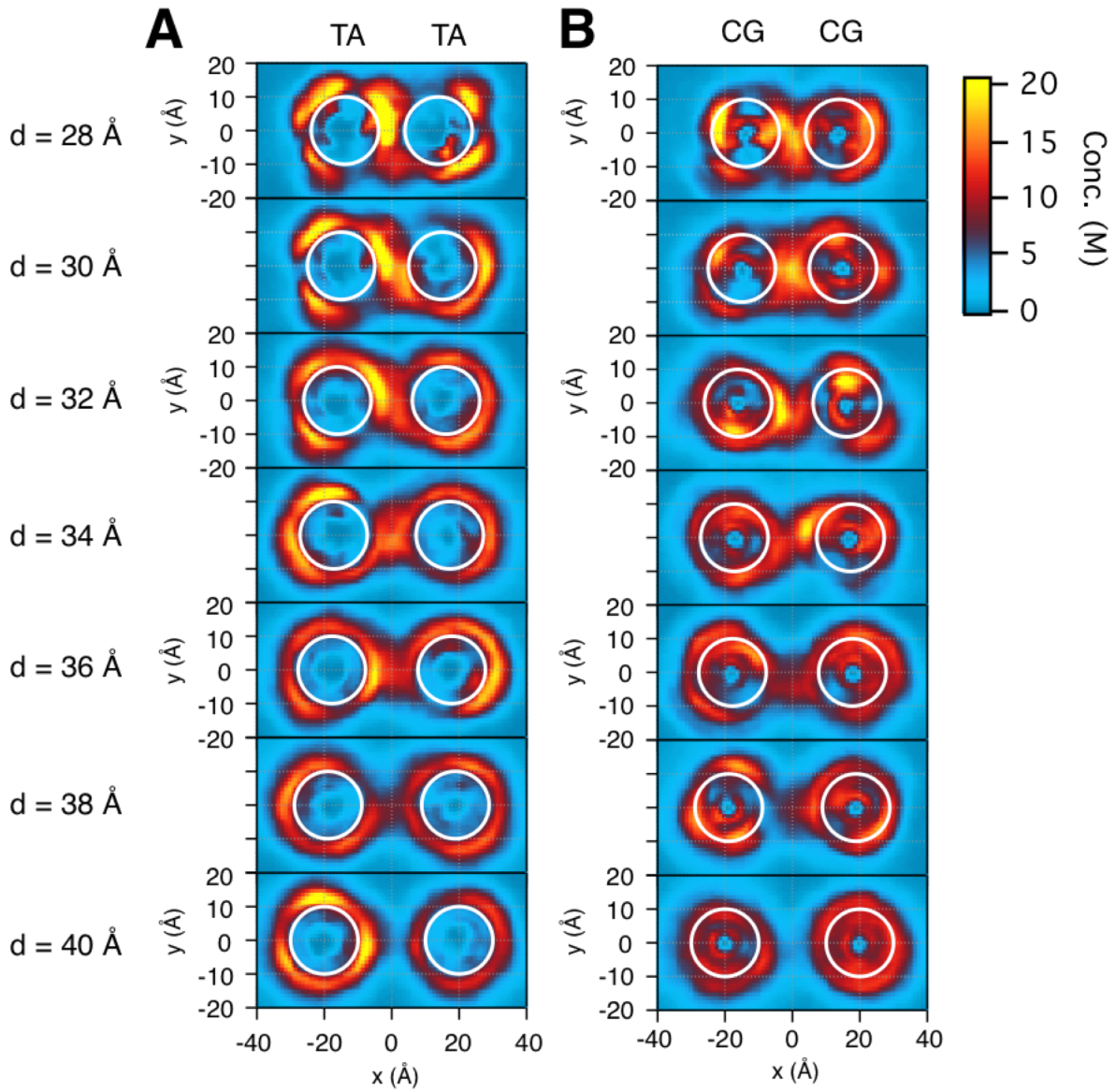


**Supplementary Figure 5.** The local concentration of $Lys_6$ heavy atoms near TA-repeat (A) or CG-repeat (B) DNA averaged over simulated time, shown as heatmaps. White circles of 1-nm radius indicate DNA helices. Respective heat maps for a range of inter-DNA distance from 28 Å to 40 Å are shown.

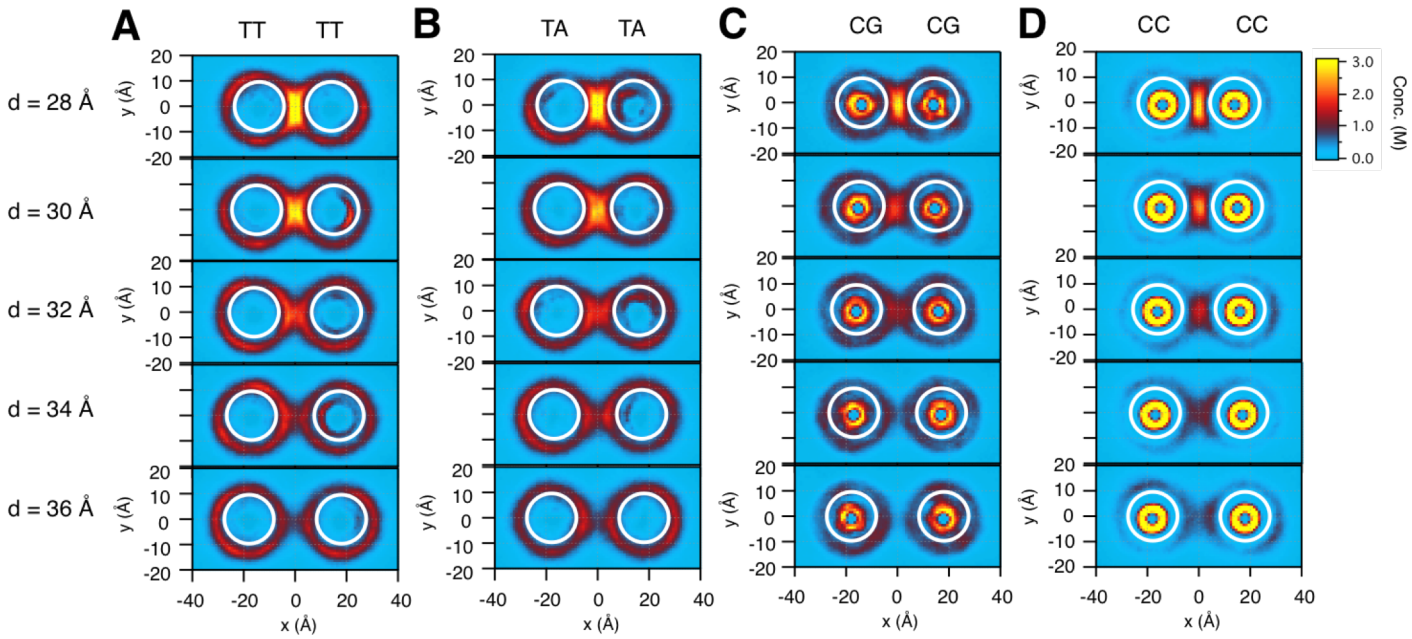


**Supplementary Figure 6.** For the MD simulations at the ratio of total spermine charge ($q^{Spm}$) to total DNA charge ($q^{DNA}$), $q^{DNA}$ / $q^{DNA}$, = 0.75, the local concentrations of spermine nitrogen atoms near TT- (A), TA- (B), CG- (C), or CC-repeat (D) DNA averaged over simulated time are shown as heatmaps. White circles of 1-nm radius indicate DNA helices. Respective heat maps for a range of inter-DNA distance from 28 Å to 36 Å are shown.

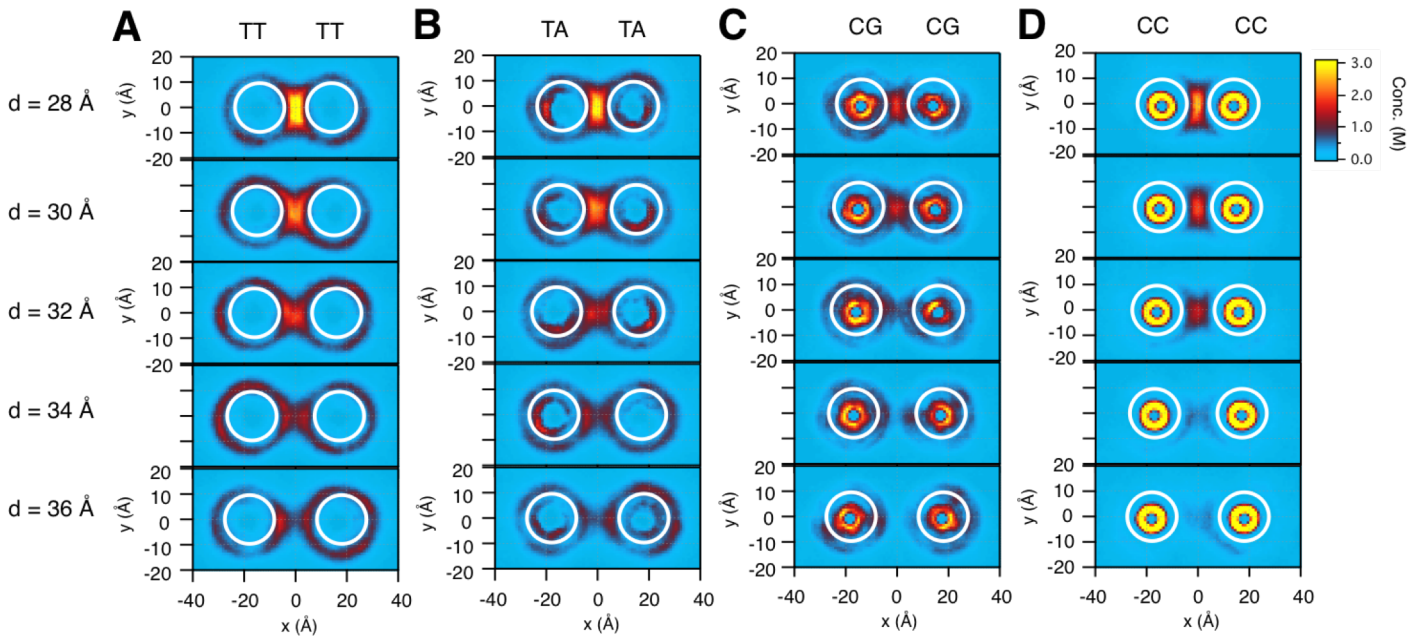


**Supplementary Figure 7.** For the MD simulations at the ratio of total spermine charge ($q^{Spm}$) to total DNA charge ($q^{DNA}$), $q^{DNA}$ / $q^{DNA}$, = 0.50, the local concentrations of spermine nitrogen atoms near TT- (A), TA- (B), CG- (C), or CC-repeat (D) DNA averaged over simulated time are shown as heatmaps. White circles of 1-nm radius indicate DNA helices. Respective heat maps for a range of inter-DNA distance from 28 Å to 36 Å are shown.

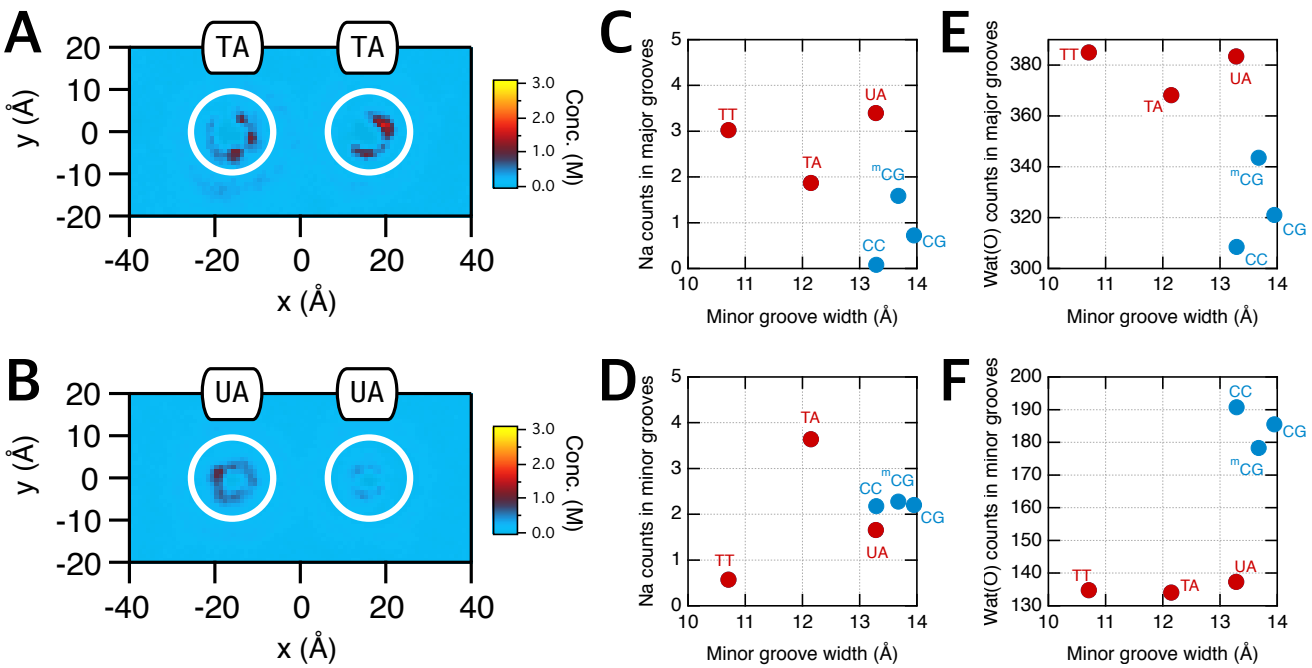


**Supplementary Figure 8. Binding of sodium ions and water molecules in grooves of DNA. (A, B)** The local concentration of sodium near TA-repeat (A) or UA-repeat (B) DNA at the inter-dsDNA distance of 32 Å averaged over simulated time, shown as heatmaps. **(C, D)** The number of sodium ions in major (C) and minor (D) grooves as a function of minor groove width. **(E, F)** The number of water oxygen atoms in major (E) and minor (F) grooves as a function of minor groove width. For panels C–F, the umbrella sampling trajectories of a pair of 20-bp DNA molecules in the presence of spermine were used. For each umbrella sampling (sequence indicated near data points), average value of all windows is shown in symbol. Standard error of window averages was smaller than the size of symbols. Atoms within 9Å from the any of DNA axes were considered to be groove-bound.

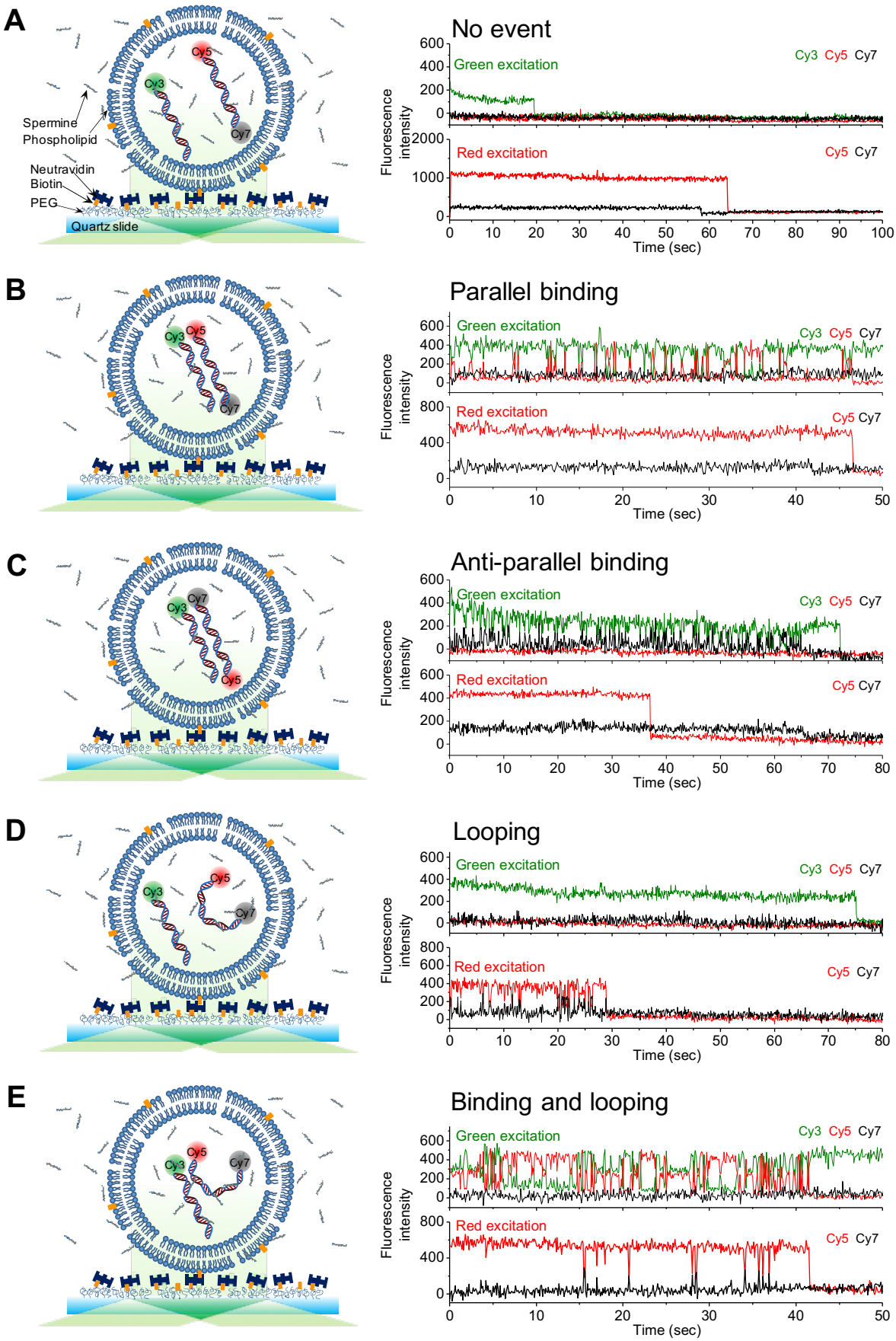


**Supplementary Figure 9.** Example three-color smFRET traces showing diverse behaviors of DNA condensation. FRET signal upon green excitation exhibit either parallel (Cy3-to-Cy5 FRET) or anti-parallel (Cy3-to-Cy7) binding and FRET signal upon red excitation exhibit looping (Cy5-to-Cy7 FRET). Schematic representation of the behaviors and corresponding example traces exhibiting no events (A), parallel binding events (B), anti-parallel binding events (C), looping events (D), and both binding and looping events (E).

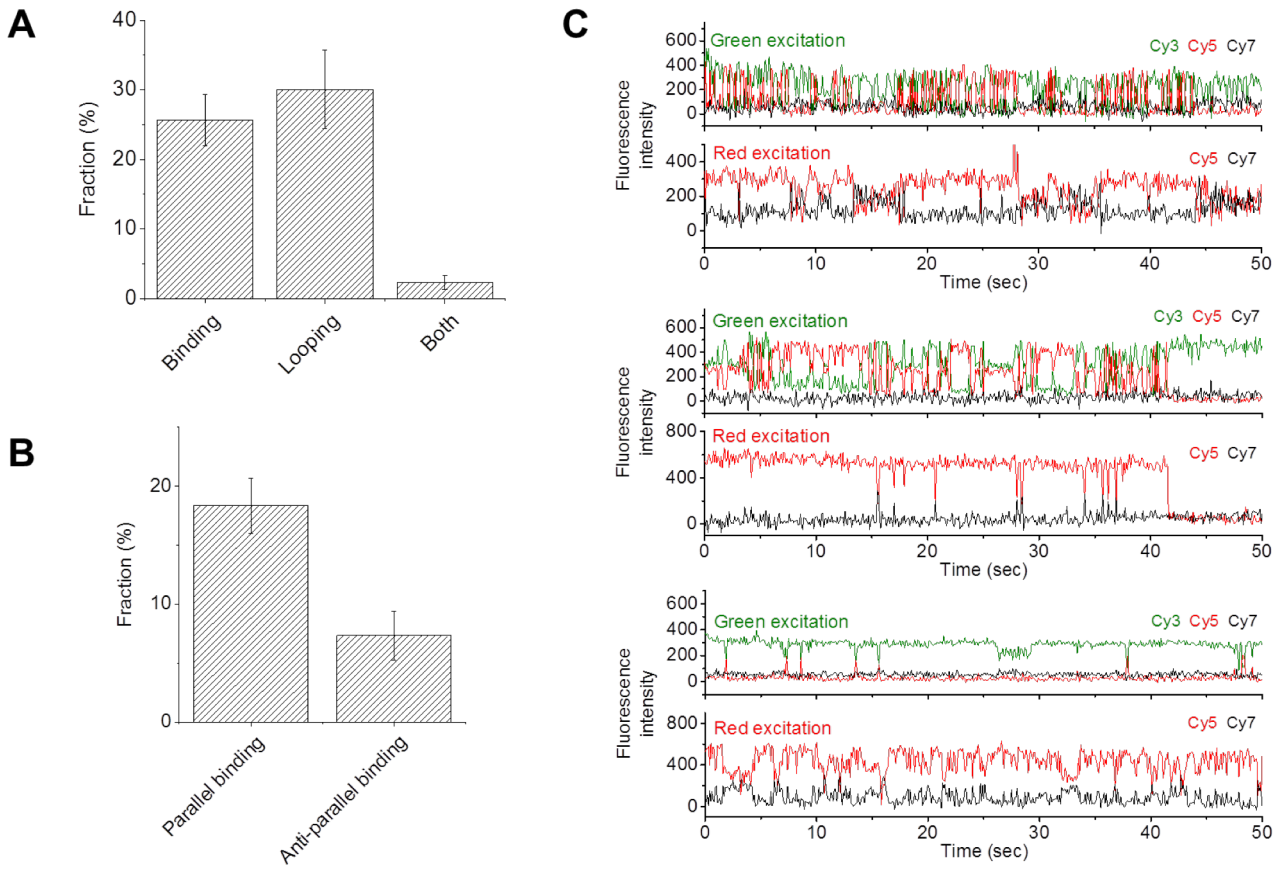


**Supplementary Figure 10.** Statistics on the frequency of binding and looping events from three-color smFRET measurements on vesicle-encapsulated pairs of 120-bp TA-rich DNA constructs with 1 mM spermine. **(A)** From three sets of single molecule measurements which produced 62, 80, and 83 traces, respectively, having all three kinds of dyes colocalzed, the percentages of traces showing binding, looping, or both events are shown. **(B)** The percentages of traces showing parallel binding and antiparallel binding events are shown. Error bars in (A) and (B) represent standard deviation between three sets of measurements. **(C)** Representative three-color traces revealing the various types of configurations between the pair of dsDNA molecules.

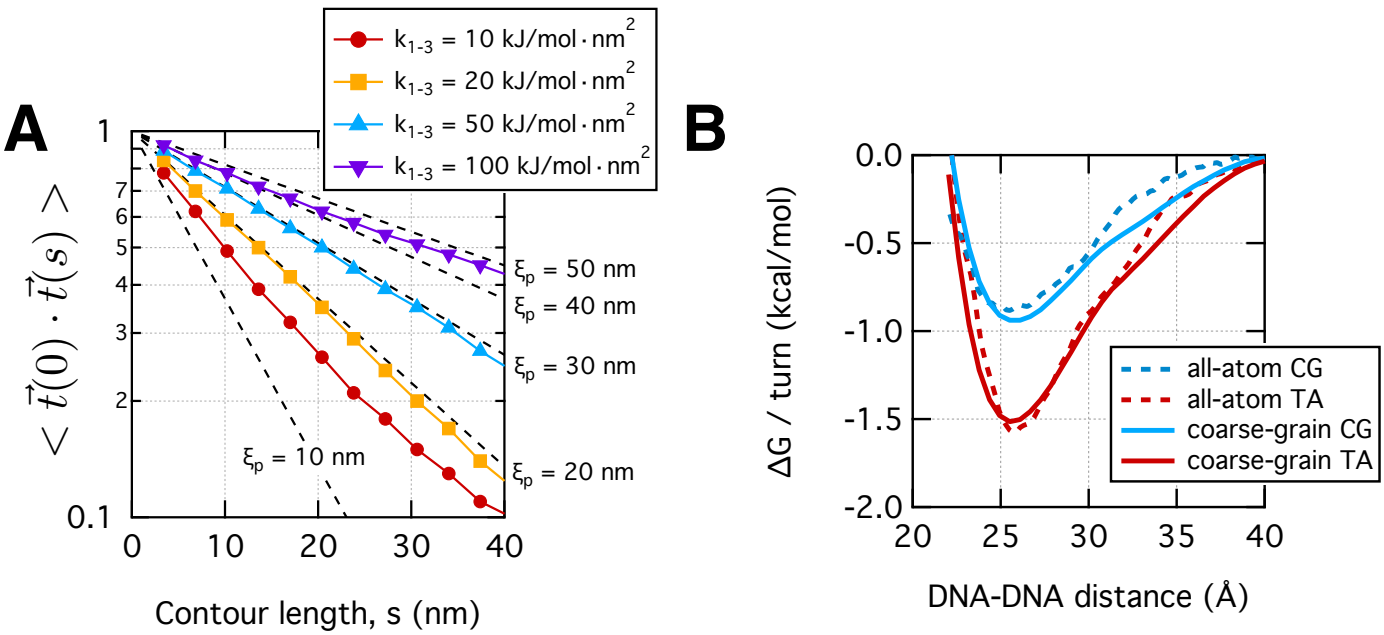


**Supplementary Figure 11.** Parameterization of the coarse-grained DNA model for the phase separation simulation. **(A)** Parameterization of the force constant for 1-3 bonded interaction ($k_{1-3}$) against persistence length ($\xi_p$). Colored marks indicate the inner product of unit tangential vectors separated by contour length *s* averaged over the 100-μs simulation of a 10,000-bp DNA. Dashed lines indicate $e^{-s/\xi p}$ for $\xi_p$ = 10, 20, 30, 40, and 50 nm. **(B)** Comparison of interaction free energy profiles between a pair of parallel dsDNA molecules using the all-atom (dashed lines) and the coarse-grained (solid lines) umbrella sampling simulations. The all-atom data for CG- and TA-repeat DNA in Sup. Fig. 4A. was used for the parameterization.